Stimuli-responsive liquid crystal elastomers for dynamic cell culture

Aditya Agrawal
Department of Chemical and Biomolecular Engineering, William Marsh Rice University, Houston, Texas 77005, USA

Oluwatomiyin Adetiba
Department of Bioengineering, William Marsh Rice University, Houston, Texas 77005, USA

Hojin Kim
Department of Chemical and Biomolecular Engineering, William Marsh Rice University, Houston, Texas 77005, USA

Huiying Chen
Department of Bioengineering, William Marsh Rice University, Houston, Texas 77005, USA

Jeffrey G. Jacot[b)]
Department of Bioengineering, William Marsh Rice University, Houston, Texas 77005, USA; and Division of Congenital Heart Surgery, Texas Children's Hospital, Congenital Heart Surgery Services, Houston, Texas 77030, USA

Rafael Verduzco[a)]
Department of Chemical and Biomolecular Engineering, William Marsh Rice University, Houston, Texas 77005, USA

(Received 7 July 2014; accepted 10 December 2014)

Responsive, biocompatible substrates are of interest for directing the maturation and function of cells in vitro during cell culture. This can potentially provide cells and tissues with desirable properties for regenerative therapies. Here, we demonstrate a straightforward and scalable approach to attach, align, and dynamically load cardiomyocytes on responsive liquid crystal elastomer (LCE) substrates. Monodomain LCEs exhibit reversible shape changes in response to cyclic heating, and when immersed in an aqueous medium on top of resistive heaters, shape changes are fast, reversible, and produce minimal temperature changes in the surroundings. We systematically characterized the strain response of LCEs in water and demonstrated the attachment and alignment of neonatal rat ventricular myocytes on LCE substrates. Cardiomyocytes attached to both static and stimulated LCE substrates, and under cyclic stimulation, cardiomyocytes aligned along the primary direction of strain. This work demonstrates the potential of LCEs as stimuli-responsive substrates for dynamic cell culture.

I. INTRODUCTION

Cellular alignment plays a key role in the properties and function of contractile tissue.[1,2] Various engineering strategies have been implemented to align, culture, and load contractile cells in vitro, including mechanical stimulation, topographical patterning, and electrical stimulation.[1,3,4] These approaches have provided insight into cellular biomechanics and tissue properties when cells are cultured in a dynamic mechanical environment and potentially provide methods to engineer tissues for repair and regenerative therapies.[5]

The importance of mechanical strain in cardiac tissue is widely recognized. Mechanical strain influences cardiomyocyte alignment, elongation, and differentiation.[1,6–8] Devices for subjecting cardiac tissue to mechanical strain during culture have been demonstrated for 2-D cell sheets[7,9,10] and 3-D scaffolds,[11–13] and commercial devices are now available for applying strain during cell culture (e.g., the Flexcell® strain apparatus). These devices are relevant to the development of cellular and tissue replacement therapies,[14] such as recent work demonstrating that cardiac cell grafts prepared in vitro can integrate with and improve the function of failing hearts.[15,16] Simpler methods for preparing aligned myocyte cell sheets are needed to advance these studies and reduce the cost of potential therapies.

Stimuli-responsive materials can potentially address the limitations of conventional devices and static materials for biomedical applications. For example, Mather et al. demonstrated the use of shape-memory polymers for dynamically changing substrate topography during and after cell culture.[17,18] Schlunck et al. implemented magnetically responsive elastomer nanocomposites for modulating substrate stiffness during cell culture.[19]

Contributing Editor: Adrian Mann
Address all correspondence to these authors.
[a)]e-mail: rafaelv@rice.edu
[b)]e-mail: jeff.jacot@rice.edu
This paper has been selected as an Invited Feature Paper.
DOI: 10.1557/jmr.2014.392

https://doi.org/10.1557/jmr.2014.392 Published online by Cambridge University Press

 © Materials Research Society 2015

Other examples include thermoresponsive and light-responsive polymer systems, as described in recent review articles.[3,20–26]

Here, we demonstrate the application of liquid crystal elastomers (LCEs) for dynamic cell culture. LCEs are stimuli-responsive polymer networks, which exhibit a fully reversible and large-amplitude shape-response.[27–29] Despite this, the implementation of LCEs for biomedical applications has been limited for a number of reasons: The nematic-to-isotropic (T_{NI}) transition temperature of LCEs is typically much higher than room temperature, the shape-response of LCEs can be slow, and LCEs are unresponsive to electric or magnetic fields in the pristine state. Here, we demonstrate that LCEs are effective as shape-responsive substrates for dynamic cell culture. LCEs are placed on a resistive heater, immersed in cell culture media, and subjected to cyclic heating. The resistive heater supplies heat locally to the LCE, and the LCE undergoes volume-conserving, uniaxial contraction and elongation with heating and cooling, respectively. Thin samples allow for operation at low heating power, resulting in fast (~1 s) shape changes with minimal ambient heating. Neonatal rat ventricular myocytes (NRVM) were cultured on shape-responsive LCEs and exhibited good attachment and viability. Under cyclic strain, NRVM show orientational ordering along the primary strain axis. This work demonstrates a simple device for dynamic cell culture and the applicability of LCEs as stimuli-responsive substrates for cell culture applications.

II. EXPERIMENTAL

A. Materials

Poly(methylhydrosiloxane) (PMHS) was purchased from Gelest and used as received. Reactive liquid crystal 4-methoxyphenyl 4-(3-butenyloxy)benzoate and catalyst dichloro(1,5-cyclooctadiene)platinum(II) were purchased from TCI America and used as received. The crosslinker (1,4-di(10-undecenyloxy)benzene) was synthesized as previously described.[30] Collagen type I (rat tail) was purchased from Corning at a concentration of 3.4–3.6 mg/mL and diluted to 50 μg/mL in 0.02 N acetic acid. Laminin was purchased from Sigma Aldrich at a concentration of 1 mg/mL and diluted to 10 μg/mL in 1x Dulbecco's Phosphate Buffered Solution (DPBS) purchased from Corning. Fibronectin (bovine plasma) was also purchased from Sigma Aldrich at a concentration of 1 mg/mL and diluted in DPBS to a concentration of 5 μg/mL. Room temperature vulcanized (RTV) medical grade silicone adhesive Silbione MED ADH 4100 was used to adhere LCEs to heaters. Poly(dimethylsiloxane) (PDMS) was prepared using a Sylgard 184 silicone elastomer kit from Dow Corning at the recommended 10:1 weight ratio of monomer:curing agent. Before use, PDMS elastomers were washed by immersion in dichloromethane to remove unreacted oligomer, followed by air drying. All solvents were purchased from commercial suppliers and used as received. Resistive Kapton flexible heaters were purchased from Omega. Resistive heaters have a heating power of 10 W/in^2 and dimensions of 1″ × 1″ (KHLV-101/10-P) or 0.5″ × 2″ (KHLV-0502/10-P).

B. Preparation of LCEs

4-Methoxyphenyl 4-(3-butenyloxy)benzoate (166.2 mg, 0.557 mmol), 1,4-di(10-undecenyloxy)benzene (12.8 mg, 0.0310 mmol), and PMHS (40 mg, M_w = 2300 g/mol) were dissolved in 0.4 mL anhydrous toluene along with 15 mL of a 1 wt% solution of platinum catalyst dichloro (1,5-cyclooctadiene)platinum(II) in dichloromethane. The reaction mixture was added to a rectangular Teflon mold (3 cm × 2 cm × 1 cm) and heated to 60 °C for 15–20 min with gentle agitation. Next, the partially crosslinked elastomer was cooled by briefly immersing the Teflon mold in liquid nitrogen, and then the LCE was carefully removed from the Teflon mold. The sample was cut to the desired dimensions and hung vertically with 6 g of weight attached to the opposite side of the LCE. The LCE was hung under load at room temperature for at least 5 days during which the crosslinking reaction completed and the LCE network was aligned. After completion of the crosslinking reaction, the LCE was immersed in toluene to remove the unreacted material and then dried in air.

C. Modification of LCEs for cell attachment

To enhance cellular attachment, the top surface of the LCE was modified by a combination of UV ozone and plasma cleaning, coating of the top surface with an inert polystyrene or gold film, and deposition of a protein layer. In a typical procedure, LCEs were cleaned by oxygen plasma (Model 1020 Fischione Instruments Plasma Cleaner) for 20 s and then coated with a 30 nm layer of gold by sputtering (Denton Desk V sputter system). The samples were then cleaned by UV ozone for 10 min (Jelight, Model 42 UVO cleaner), soaked in 70% alcohol, and washed with PBS before a solution of collagen type I with a concentration of 50 μg/mL in 0.02 N acetic acid was applied to the gold-coated LCE surface. A drop of the collagen solution was placed on the LCE to cover the entire surface. This was left for 2 h at room temperature or overnight at 4 °C. Afterward, the LCE was preconditioned in an incubator at 37 °C and 5% CO_2 for a minimum of 1 h before cell seeding. In modified procedures, a 1 mg/mL solution of fibronectin or a 10 μg/mL solution of laminin was deposited on the LCE instead of collagen. As an alternative to gold, a thin polystyrene (PS) film can be deposited on the LCE

https://doi.org/10.1557/jmr.2014.392 Published online by Cambridge University Press

surface by spin-casting onto silicon and transferring the PS film to the LCE surface, as described previously.[31]

D. Cell culture with NRVM

NRVM were harvested from freshly dissected ventricles of 1- to 3-day-old Sprague-Dawley rats using an isolation kit (Cellutron, Highland Park, NJ). Cells were isolated using the Cellutron myocyte isolation protocol. After isolation, cells were resuspended in high-serum plating media (Dulbecco's Modified Eagle Media (DMEM), 17% M199, 10% horse serum (HS), 5% fetal bovine serum (FBS), 100 units/mL penicillin, and 50 mg/mL streptomycin) and plated on top of LCE substrates prepared as described above at a density of 100,000–600,000 cells/cm^2. Around 24 h later, cells were transferred to low-serum maintenance media (DMEM, 18.5% M199, 5% HS, 1% FBS, and antibiotics). LCEs were then subjected to cyclic heating. Resistive heaters were turned on and off through the use of a Myopacer (Ionotopics) field stimulator and time relay. The system can supply AC (0.010–99 Hz) voltages in the range of 0–40 V with pulse durations (equal on and off times) of 0.6 s–24 h. Cell cultures were maintained inside an incubator at 37 °C and 5% CO_2 and fresh maintenance media were added every 1–2 days. All culture media were purchased from Invitrogen and sera were purchased from Gemini BioProducts.

E. Cell staining and analysis

To determine the cell attachment and viability, the cells were stained using a viability/cytotoxicity assay kit from Biotium (product number 30002-T) and left at room temperature for 30 min. They were then imaged and counted using an Image J (NIH) cell counter. To outline the membrane of the cell, the cells were stained using calcein AM (Biotium). For nuclei staining, the cells were covered with VectaShield DAPI-containing mounting medium (Vector Labs) before being imaged under a fluorescent microscope (Leica). All cell count numbers reported are over a 0.36 mm^2 area.

III. RESULTS AND DISCUSSION

Our experimental configuration for cell culture studies with LCE substrates is shown in Fig. 1. Monodomain LCEs were prepared through a two-step crosslinking method,[32] with some modifications (see the Experimental section for detailed procedure). The LCEs prepared for this study were polysiloxane based side-group LCEs, and the final samples were rectangular with a length L of 10 mm, a width W of 5 mm, and a thickness H of 0.5 mm. For use in cell culture, the LCE surface was modified to enhance cell attachment, placed on top of a resistive heater and immersed in cell culture media. The entire system was kept in a temperature controlled incubator held at 37 °C. Heat supplied transiently to the bottom LCE surface results in bulk LCE temperature changes, which leads to reversible, volume-conserving, uniaxial elongation and contraction of the LCE sample during cell culture. The heating power and on/off pulse durations were tuned to achieve a desired strain and frequency and to minimize ambient heating. Below, we discuss the shape-response of LCEs in water before

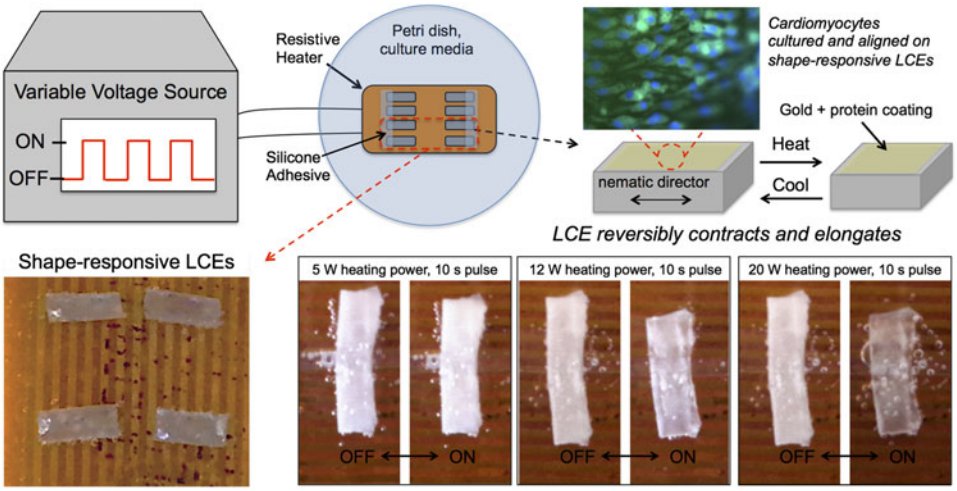


FIG. 1. Schematic of experimental configuration for dynamic cell culture (top) and photographs of LCEs on resistive heaters. A variable voltage supplied to the resistive heaters resulted in cyclic heating of the LCE substrates. The LCE substrates and resistive heaters were fully covered by culture media, and LCEs were held in place by a medical grade silicone adhesive. The Petri dish and culture media resided in an incubator maintained at 37 °C and 5% CO_2. For the images on the bottom-right side, the same LCE was analyzed at different heating powers and at 10 s pulse duration (10 s on, 10 s off). The LCE was held in place by silicone adhesive. Images were taken after 10 min of cyclic heating for equilibration, and the LCE sample shown was approximately 9 mm in length.

https://doi.org/10.1557/jmr.2014.392 Published online by Cambridge University Press

presenting the results of culturing NRVM on shape-responsive LCEs.

The response of the LCEs to transient heating can be predicted through simple physical arguments based on energy conservation and known physical properties of the LCEs. The LCE samples were rectangular with a thickness of 500 μm and a total volume V of 0.025 cm^3. The density, heat capacity, and thermal conductivity of the LCE are approximated to be that of PDMS, which has a density ρ of 0.97 kg/m^3, a heat capacity C_p of 1460 J/kg K, and a thermal conductivity k of 0.15 W/m K.[33] LCEs contract spontaneously by 35% when heated from room temperature to the nematic-to-isotropic transition temperature (T_{NI}),[31,34] and the LCEs studied have a T_{NI} of approximately 75 °C measured by differential scanning calorimetry. Based on these values, the amount of heat required to raise the bulk temperature of the LCE from 37 °C to the T_{NI} (75 °C) is $\rho V C_p \Delta T$, or approximately 1.8 J. Thus, small amounts of heat, supplied locally to the LCE, can provide significant bulk temperature changes and macroscopic shape-changes in the LCE.

Under transient heating, the bulk temperature of the LCE will vary as the external heating source is turned on and off and heat is dissipated to the surroundings. Assuming that heat is dissipated quickly at the surface of the LCE in contact with water, the characteristic time scale for bulk temperature changes (and therefore sample strains) is set by thermal diffusion through the thickness of the LCE, $\sim \rho C_p H^2/k$, or roughly 2 s for the present samples. Thinner LCE samples or LCEs with higher thermal conductivities respond more quickly. This simple analysis predicts that local heating of LCEs can produce bulk temperature changes and therefore macroscopic sample strains (up to 35%) on timescales on the order of ~2 s with low amounts of heat (~1.5 J). These strains and timescales are comparable to the strains and frequencies used to align cells by mechanical deformation of a substrate or scaffold.[1]

As shown in Fig. 1 and in videos available as Supplementary Materials, monodomain LCEs placed on a resistive heater with 5–20 W heating power and 1–10 s pulse duration contract and elongate reversibly in water. LCEs reach steady state after several minutes of cycling and exhibit fully reversible strain in response to transient heating. The magnitude of the reversible strain depends on both the heating power and the pulse duration. Higher heating powers or longer pulse durations result in larger changes in the bulk LCE temperature and therefore larger strains. In all cases, the strain is fully reversible. Monodomain LCEs are typically transparent due to uniform alignment of the nematic director.[29] Our monodomain LCEs are transparent after preparation, but as can be seen in Fig. 1, LCEs become hazy over time when placed in water. This may be due to water penetration or material degradation at the interface with water. However, this does not have an impact on the shape-response of LCEs, and the LCEs are observed to exhibit a reversible shape response for the duration of our experiments, typically several days.

To gain a more quantitative understanding of the reversible shape response of LCEs under water, the reversible strain was measured for varying pulse durations and heating powers. The response of LCEs to cyclic on/off heating pulses at varying heating powers is shown in Fig. 2. Strains were measured by recording the videos of the shape response and analyzing the images. For low heating powers, the reversible strain was roughly 5% even for long pulse durations, but at higher heating powers reversible strains as high as 35% were recorded. The maximum strain is comparable to that measured for LCEs heated in air.[31,34] For short pulse durations (0.6 s), all LCEs exhibited less than 1% strain. At these short pulse durations, heat was dissipated quickly and the bulk LCE temperature remained relatively constant. At 1 s pulse durations, up to 4% reversible strain was achieved with 20 W heating power. In comparison to experiments performed in water at 5 W, samples in air exhibited higher strain values in response to cyclic heating. This is expected due to the faster heat dissipation in water, which results in lower bulk temperature fluctuations in LCEs. These measurements demonstrate that LCEs can respond reversibly in water, and the response time and strain can be tuned by varying the heating power and pulse duration. Videos demonstrating the response of LCEs in air and under water on top of resistive heaters are provided with supplementary materials available online.

The LCE bulk and surface temperature and the temperature in the ambient media are important for the proposed application. Variations in the bulk LCE temperature give rise to macroscopic strains (shown in Fig. 2), and, ideally, the surface and media temperatures

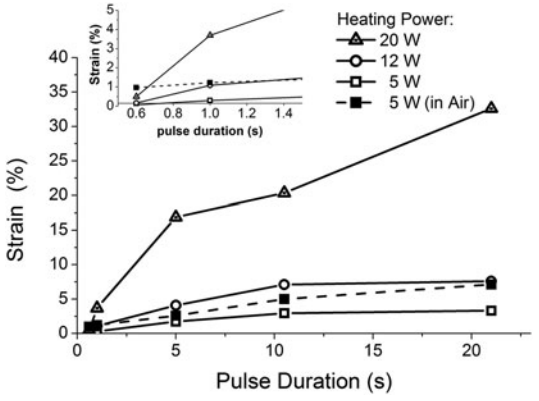


FIG. 2. Plot of reversible strain in LCEs as a function of heating power and pulse duration. Reversible strain was determined by measuring the maximum and minimum sample lengths during heat cycling. All samples were analyzed in water, except where indicated. The inset shows the strain measured for pulse durations shorter than 1.5 s.

https://doi.org/10.1557/jmr.2014.392 Published online by Cambridge University Press

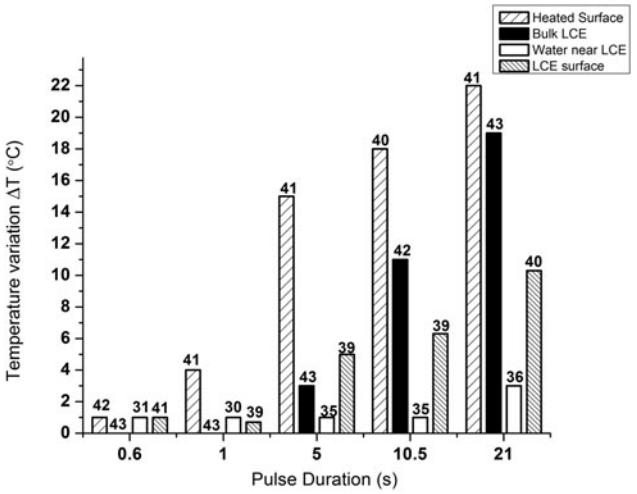


FIG. 3. Temperature variation near the surface of the resistive heater, in the bulk LCE, near the LCE surface and on the LCE surface for cyclic heating with 12 W heating power. All measurements were made using a thermocouple, except for the LCE surface which was measured using an IR probe, as described in the main text. The values above each bar indicate the average temperature (°C) for each case. All samples were allowed to equilibrate for at least 10 min under cyclic heating. The ambient temperature was approximately 25 °C. Data for 5 and 20 W under similar experimental conditions are provided in the Supporting Information.

should remain in a temperature range to ensure viability of cells on the LCE surface. A temperature gradient from the bottom of the LCE to the top surface is essential to producing macroscopic strains while maintaining moderate temperatures at the top surface. At the same time, too steep of a temperature gradient would lead to curling or buckling of the sample instead of uniaxial elongation and contraction. The LCE bulk temperature was monitored by incorporating a thermocouple into the LCE. We also monitored the temperature near the surface of the resistive heater, near the top surface of the LCE, and in the media far from the heater and LCE using a thermocouple. Obtaining an estimate of the temperature of the LCE surface in water presented practical difficulties as our measurements using a thermocouple matched those of the water near the LCE surface. To get an estimate of the LCE surface temperature, the sample was allowed to equilibrate under cyclic heating for at least 10 min, then water was removed from the dish until the level of water was below the top surface of the LCE. An IR probe (Model IRT0421Kintrex, Vienna, VA) then provided a measure of the temperature of the top surface, although we expect this value to be lower when the LCE is kept completely immersed in water.

As shown in Fig. 3 for 12 W heating power, the temperature near the resistive heater varied substantially for pulse durations of 5 s and greater, by up to 20 °C between on and off pulses. The LCE bulk temperature fluctuated by almost as much at long pulse durations, but at 5 s pulse durations and shorter the bulk LCE temperature varied by only roughly 3 °C. The temperature near the LCE surface fluctuated substantially less than the bulk LCE temperature, even at long pulse durations, and the average temperature of the top surface of the LCE was always less than that of the bulk LCE. Our measurements thus indicate a temperature gradient across the sample (from the bottom to top surface), with a 5–10 °C difference in temperature between the maximum temperatures of the top LCE surface and the bulk LCE during cyclic heating. At the same time, no buckling or curling is observed during cyclic heating. The measurements also show that at shorter pulse durations, heat dissipation at the LCE surface is effective at maintaining moderate temperatures at the surface where cells can attach to the LCE. The temperature of the water in the Petri dish far from the LCE surface and resistive heaters remained at ambient. Data for 5 and 20 W heating powers are provided in the Supporting Information Figures S1 and S2, respectively.

The results presented above indicate that LCEs may be effective for cell culture at lower pulse durations and heating powers. To implement LCEs for use in cell culture, the top surface was modified to allow cell attachment. Polysiloxane elastomers like PDMS and LCEs have low surface and adhesion energies and are not amenable to cellular attachment. Before carrying out dynamic cell culture experiments, potential coatings were tested on PDMS elastomers to determine the most viable for myocyte attachment. PDMS was used as the test substrate because it is readily available, easily synthesized in large quantities and has a similar molecular chemical structure to our LCEs. To modify the surface, a thin layer of polystyrene (PS) was deposited on PDMS, the surface of the PDMS-PS bilayer was subjected to UV-ozone or plasma cleaning, and finally the treated bilayer was coated with one of three different proteins: collagen, fibrinogen or laminin. These treated PDMS-PS elastomers were then used to culture NRVM. Cell viability was analyzed by live-dead assays (calcein AM/EthD III staining). Tissue-culture plastic and untreated PS-PDMS elastomers were used as positive and negative controls, respectively.

As shown in Fig. 4, protein layers exhibited improved NRVM attachment and viability compared with PS-PDMS negative control but reduced viability compared with tissue-culture plastic. No significant difference is observed in NRVM viability between the different protein samples, but our experiments indicate reduced consistency of cell attachment on surfaces treated with fibrinogen and laminin compared with collagen. Collagen was used as the protein coating for all studies described below.

The results above indicate that a PS-collagen coating provides reliable cell attachment and viability. However,

https://doi.org/10.1557/jmr.2014.392 Published online by Cambridge University Press

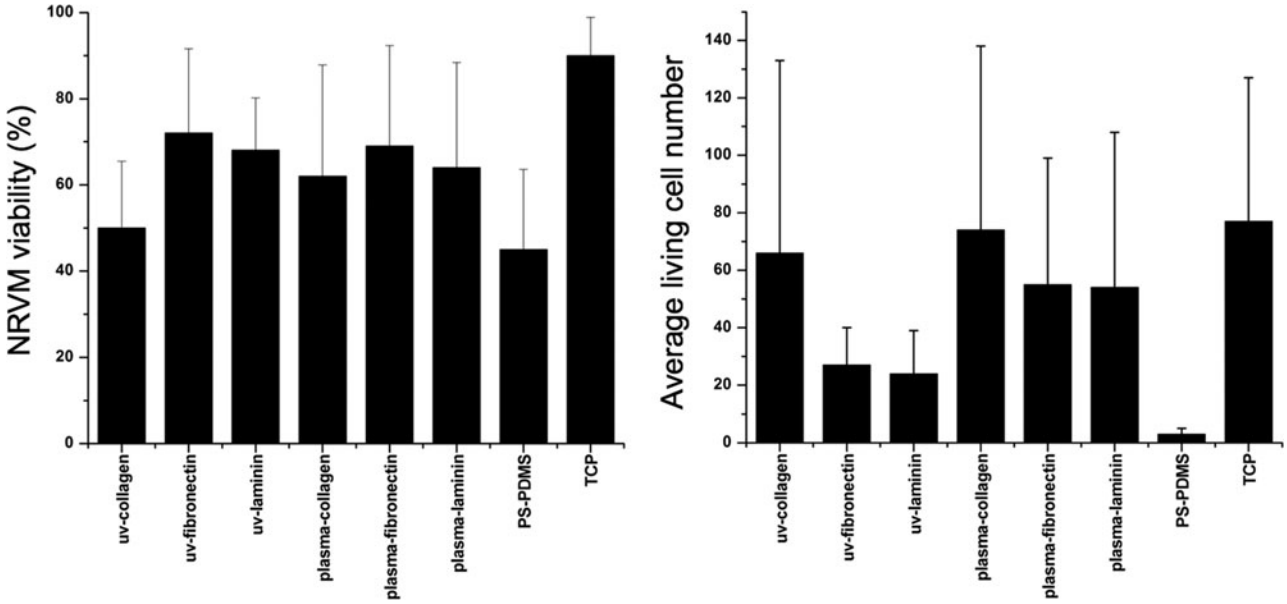


FIG. 4. NRVM viability (left) and number of live cells attached (right) on PDMS-PS elastomers with different surface treatments. Three proteins and two cleaning procedures were tested. Cell numbers reported per 0.36 mm^2 area.

a significant drawback of using PS coatings is difficulty in applying it to several samples. PS films are deposited on LCE surfaces through film transfer,[31] which requires casting, lifting off, and transferring a PS film to each LCE. As a more scalable approach, we explored the modification of LCEs using gold. Gold is easily deposited on multiple LCE samples simultaneously using a sputter coater and can be subsequently modified with collagen to enhance cellular attachment. The use of PS coatings may be of interest to others in the field, and in the Supporting Information we provide an example image of myocytes cultured on PS-coated LCEs (Figure S3). We observe good cell attachment and viability on these surfaces.

To prepare gold-LCE and gold-PDMS bilayers, the elastomers are treated with oxygen plasma before a thin, inert gold layer (30 nm) is deposited on LCEs or PDMS by sputter coating. Gold is easily deposited on multiple samples simultaneously using a sputter coater. Next, the surfaces were cleaned by UV-ozone, and collagen was deposited on the surfaces. Since silicone elastomers are known to undergo time-dependent changes of surface chemistry, we tested the effect of applying collagen immediately after UV-ozone cleaning and after waiting 16 h before applying collagen to the surface. NRVM were then cultured on the substrates, and the resulting surfaces were analyzed for cell viability and attachment.

Both PDMS and LCE elastomers modified by gold and collagen treatment exhibited high NRVM viability [see Fig. 5]. A larger number of cells were found to attach to LCEs compared with PDMS, and a drop in cell attachment was observed for both elastomers when waiting 16 h in between UV-ozone treatment and collagen

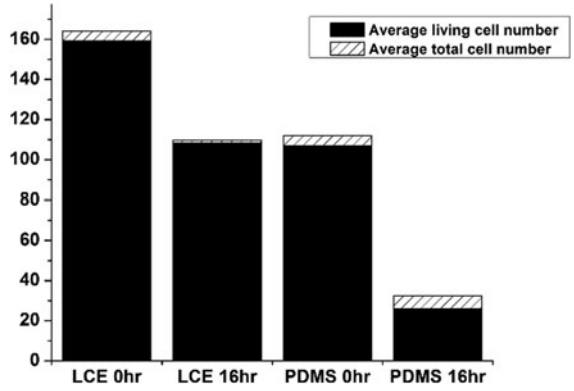


FIG. 5. NRVM live and total cell numbers on gold-modified LCE and PDMS samples. All elastomers were modified through deposition of a 30 nm gold layer followed by UV-ozone cleaning and deposition of collagen. Collagen was deposited either immediately after UV-ozone treatment (0 h) or 16 h after UV-ozone treatment. Standard deviations are for living cell numbers. Cell numbers reported per 0.36 mm^2 area.

deposition. This suggests that surface chemistry changes or the adsorption of contaminants over this time period may affect collagen deposition on the gold-coated elastomer surfaces. Representative live-dead assays from both PDMS and LCEs are shown in Fig. 6, showing high NRVM viability (greater than 95%).

Next, we tested cell attachment, viability, and orientation on LCEs subjected to cyclic heating. It should be noted that the deposition of a thin gold layer does not affect the macroscopic strain of the LCEs but can affect the surface topography. Gold-coated LCEs are expected to exhibit aligned surface wrinkles that disappear and reappear depending on sample strain. This reversible

https://doi.org/10.1557/jmr.2014.392 Published online by Cambridge University Press

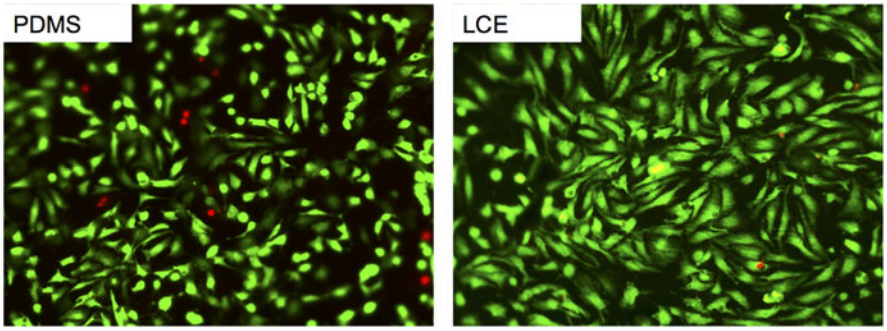


FIG. 6. Calcein AM stained images of cardiomyocytes on PDMS (left) and LCE (right). Surfaces were treated by gold deposition and collagen in both cases. Live cells were pseudocolored green and dead cells red.

surface wrinkling in LCEs has been previously demonstrated and studied by our laboratory.[31]

Prior work with cardiomyocytes has explored a range of strain and strain frequencies.[1] Early work demonstrating the use of silicone membranes for strain-induced alignment of cardiomyocytes typically applied 20% strains.[35,36] However, a more recent study found comparable increase in the force of contraction for engineered heart tissue subjected to strains of 4–20%,[37] and cardiomyocyte remodeling and sarcomere addition have been observed at 10% strains.[38,39] For this study, we chose a strain of 5% and pulse duration of 6.5 s. This was chosen due in part to our temperature measurements which indicate that at 12 W heating power, excessive heating of the LCE and ambient are avoided. However, it is recognized that this strain and frequency are likely not be optimal for myocyte alignment. Future work will explore the role of varying strain and strain frequency and also seek to increase maximum strain while minimizing ambient heating.

NRVM were cultured on LCEs under static conditions for 24 h, and then cyclic heating was initiated continuously for 2–3 days. Cells were then stained for analysis. As shown in Fig. 7, cells successfully attached on LCEs subjected to cyclic heating. The density of cells attached to the surface was substantial, even under cyclic heating. Some samples also showed evidence for cell connectivity and network formation (see Supporting Information Figure S4). Viability and total cell counts were difficult to quantify due to the high density of cells, but nuclei staining confirmed that cells attached to the surface, some of which are elongated and some spherical in shape.

Cellular orientation was quantified through image analysis. We analyzed cellular orientation on static LCE and PDMS substrates and on stimulated LCE substrates [see Fig. 8]. As expected, cells cultured on static LCE and PDMS substrates are oriented isotropically. In the case of stimulated LCE substrates, some regions of the LCEs showed evidence for significant myocyte alignment. Interestingly, the preferred orientation was found to be at a slight angle relative to the major axis of the LCE. This may indicate imperfect alignment of the LCE or nonuniform deformation. Some regions of the LCE surface exhibited poorer alignment, and cells in poorly aligned regions have a slight preference for orientations parallel or perpendicular to the major strain axis. It is unclear whether heterogeneity in the quality of cellular alignment is due to nonuniform sample strain, inhomogeneities on the surface, or some other disturbance during culturing and analysis. Further studies are needed to optimize LCE stimulation to improve cellular response and orientation.

The results presented demonstrate that LCEs can be implemented as shape-responsive substrates for cell culture in a simple device configuration. Heat can be used as a stimulus to produce reversible shape changes of 1–5% and frequencies of 1.6 Hz or smaller. The cell culture data presented indicate that cells remain viable and attach to the surface of the LCE during cyclic heating/straining. Studies are underway to determine the range of strains and frequencies possible with shape-responsive LCE substrates. Future measurements will focus on more accurately measuring surface temperatures and strains and optimizing the heating power and cycle durations for improved cell alignment. We may find, for example, that cells remain viable at higher heating powers, enabling larger strains and/or shorter pulse durations. We will also analyze the properties of myocyte cell sheets grown in vitro on responsive LCE substrates to determine if cyclic strain on LCEs provides similar enhancements of tissue properties as observed on mechanically stretched elastomer surfaces.[7]

While a relatively simple device configuration was used in the present work, the same procedures reported here can be combined with innovative strategies for achieving a stimulus–response in LCEs. For example, conductive LCE nanocomposites can respond directly to electrical stimulation and localized heating.[40–42] Dye-doped LCEs or carbon-nanotube LCE nanocomposites respond to light and/or IR-radiation,[43–46] enabling

https://doi.org/10.1557/jmr.2014.392 Published online by Cambridge University Press

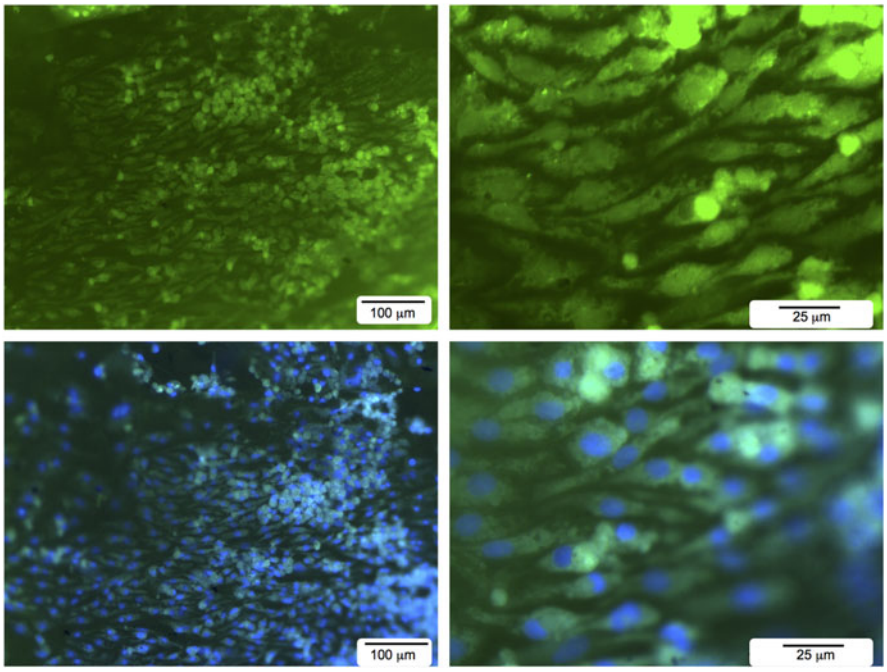


FIG. 7. Calcein AM (top) and calcein AM and DAPI (bottom) stained images of cardiomyocytes on selected regions of LCE under cyclic heating. LCEs were stimulated through 12 W heating power and 6.5 s pulse duration, producing approximately 5% uniaxial strains during cell culture. The primary strain direction is horizontal in the images above. Images are at 10x (left) and 40x (right) magnification. The cells were stained using calcein AM (Biotium) while the nuclei were stained with VectaShield DAPI-containing mounting medium (Vector Lab). The images were then observed and imaged using a fluorescent microscope.

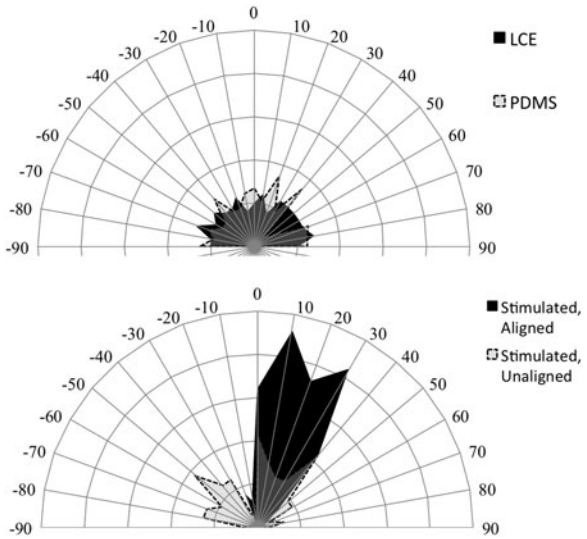


FIG. 8. Radial plots showing the orientation of cells after cell culture under static (top) and dynamic (bottom) conditions. Each radial arc represents 5% of cells counted. Under static conditions, no preferential cell orientation is observed. Under dynamic conditions, cells are preferentially oriented along the direction of elongation/contraction.

remote activation with no physical contact to a heating element or electrode. Other opportunities include using the combination of surface wrinkling[3,31] with macroscopic strains to engineer aligned cellular constructs.

ACKNOWLEDGMENTS

This work was supported by the John S. Dunn Foundation, the IBB Hamill Innovation Grant (to RV), the American Heart Association (BGIA to JGJ), the National Science Foundation (CAREER CBET-1055942 to JGJ and CBET-1336073 to RV), the National Institutes of Health/National Heart, Lung and Blood Institute (1R21HL110330 to JGJ), Louis and Peaches Owen and Texas Children's Hospital.

REFERENCES

1. Y. Li, G. Huang, X. Zhang, L. Wang, Y. Du, T.J. Lu, and F. Xu: Engineering cell alignment in vitro. *Biotechnol. Adv.* **32**, 347 (2014).
2. P. Helm, M.F. Beg, M.I. Miller, and R.L. Winslow: Measuring and mapping cardiac fiber and laminar architecture using diffusion tensor MR imaging. *Ann. N. Y. Acad. Sci.* **1047**, 296 (2005).
3. M. Nikkhah, F. Edalat, S. Manoucheri, and A. Khademhosseini: Engineering microscale topographies to control the cell–substrate interface. *Biomaterials* **33**, 5230 (2012).
4. C. Neidlinger-Wilke, E.S. Grood, J.H-C. Wang, R.A. Brand, and L. Claes: Cell alignment is induced by cyclic changes in cell length: Studies of cells grown in cyclically stretched substrates. *J. Orthop. Res.* **19**, 286 (2001).
5. F. Berthiaume, T.J. Maguire, and M.L. Yarmush: Tissue engineering and regenerative medicine: History, progress, and challenges. *Annu. Rev. Chem. Biomol. Eng.* **2**, 403 (2011).
6. T. Eschenhagen and W.H. Zimmermann: Engineering myocardial tissue. *Circ. Res.* **97**, 1220 (2005).

https://doi.org/10.1557/jmr.2014.392 Published online by Cambridge University Press

7. W-H. Zimmermann, K. Schneiderbanger, P. Schubert, M. Didié, F. Münzel, J.F. Heubach, S. Kostin, W.L. Neuhuber, and T. Eschenhagen: Tissue engineering of a differentiated cardiac muscle construct. *Circ. Res.* **90**, 223 (2002).
8. L.D. Black, J.D. Meyers, J.S. Weinbaum, Y.A. Shvelidze, and R.T. Tranquillo: Cell-induced alignment augments twitch force in fibrin gel-based engineered myocardium via gap junction modification. *Tissue Eng., Part A* **15**, 3099 (2009).
9. A.A. Lee, T. Delhaas, L.K. Waldman, D.A. MacKenna, F.J. Villarreal, and A.D. McCulloch: An equibiaxial strain system for cultured cells. *Am. J. Physiol.: Cell Physiol.* **271**, C1400 (1996).
10. S.M. Gopalan, C. Flaim, S.N. Bhatia, M. Hoshijima, R. Knoell, K.R. Chien, J.H. Omens, and A.D. McCulloch: Anisotropic stretch-induced hypertrophy in neonatal ventricular myocytes micropatterned on deformable elastomers. *Biotechnol. Bioeng.* **81**, 578 (2003).
11. J. Garvin, J. Qi, M. Maloney, and A.J. Banes: Novel system for engineering bioartificial tendons and application of mechanical load. *Tissue Eng.* **9**, 967 (2003).
12. Y. Pang, X. Wang, D. Lee, and H.P. Greisler: Dynamic quantitative visualization of single cell alignment and migration and matrix remodeling in 3-D collagen hydrogels under mechanical force. *Biomaterials* **32**, 3776 (2011).
13. J. Guan, F. Wang, Z. Li, J. Chen, X. Guo, J. Liao, and N.I. Moldovan: The stimulation of the cardiac differentiation of mesenchymal stem cells in tissue constructs that mimic myocardium structure and biomechanics. *Biomaterials* **32**, 5568 (2011).
14. M.Y. Emmert, R.W. Hitchcock, and S.P. Hoerstrup: Cell therapy, 3D culture systems and tissue engineering for cardiac regeneration. *Adv. Drug Delivery Rev.* **69–70**, 254 (2014).
15. A. Furuta, S. Miyoshi, Y. Itabashi, T. Shimizu, S. Kira, K. Hayakawa, N. Nishiyama, K. Tanimoto, Y. Hagiwara, T. Satoh, K. Fukuda, T. Okano, and S. Ogawa: Pulsatile cardiac tissue grafts using a novel three-dimensional cell sheet manipulation technique functionally integrates with the host heart, in vivo. *Circ. Res.* **98**, 705 (2006).
16. Y. Sawa, S. Miyagawa, T. Sakaguchi, T. Fujita, A. Matsuyama, A. Saito, T. Shimizu, and T. Okano: Tissue engineered myoblast sheets improved cardiac function sufficiently to discontinue LVAS in a patient with DCM: Report of a case. *Surg. Today* **42**, 181 (2012).
17. K.A. Davis, K.A. Burke, P.T. Mather, and J.H. Henderson: Dynamic cell behavior on shape memory polymer substrates. *Biomaterials* **32**, 2285 (2011).
18. P. Yang, R.M. Baker, J.H. Henderson, and P.T. Mather: In vitro wrinkle formation via shape memory dynamically aligns adherent cells. *Soft Matter* **9**, 4705 (2013).
19. M. Mayer, R. Rabindranath, J. Börner, E. Hörner, A. Bentz, J. Salgado, H. Han, H. Böse, J. Probst, M. Shamonin, G.J. Monkman, and G. Schlunck: Ultra-soft PDMS-based magnetoactive elastomers as dynamic cell culture substrata. *PLoS One* **8**, e76196 (2013).
20. P.T. Mather, X. Luo, and I.A. Rousseau: Shape memory polymer research. *Annu. Rev. Mater. Res.* **39**, 445 (2009).
21. W. Small, IV, P. Singhal, T.S. Wilson, and D.J. Maitland: Biomedical applications of thermally activated shape memory polymers. *J. Mater. Chem.* **20**, 3356 (2010).
22. D. Rickert, A. Lendlein, I. Peters, M.A. Moses, and R-P. Franke: Biocompatibility testing of novel multifunctional polymeric biomaterials for tissue engineering applications in head and neck surgery: An overview. *Eur. Arch. Oto-Rhino-Laryngol Head Neck* **263**, 215 (2006).
23. Q. Chen, S. Liang, and G.A. Thouas: Elastomeric biomaterials for tissue engineering. *Prog. Polym. Sci.* **38**, 584 (2013).
24. J.F. Mano: Stimuli-responsive polymeric systems for biomedical applications. *Adv. Eng. Mater.* **10**, 515 (2008).
25. D. Ratna and J. Karger-Kocsis: Recent advances in shape memory polymers and composites: A review. *J. Mater. Sci.* **43**, 254 (2008).
26. J. Biggs, K. Danielmeier, J. Hitzbleck, J. Krause, T. Kridl, S. Nowak, E. Orselli, X. Quan, D. Schapeler, W. Sutherland, and J. Wagner: Electroactive polymers: Developments of and perspectives for dielectric elastomers. *Angew. Chem., Int. Ed.* **52**, 9409 (2013).
27. M. Warner and E.M. Terentjev: *Liquid Crystal Elastomers* (Oxford University Press, Oxford, England, 2003).
28. H. Jiang, C. Li, and X. Huang: Actuators based on liquid crystalline elastomer materials. *Nanoscale* **5**, 5225 (2013).
29. C. Ohm, M. Brehmer, and R. Zentel: Liquid crystalline elastomers as actuators and sensors. *Adv. Mater.* **22**, 3366 (2010).
30. S.A. Ali, H.A. Al-Muallem, S.U. Rahman, and M.T. Saeed: Bis-isoxazolidines: A new class of corrosion inhibitors of mild steel in acidic media. *Corros. Sci.* **50**, 3070 (2008).
31. A. Agrawal, P. Luchette, P. Palffy-Muhoray, S.L. Biswal, W.G. Chapman, and R. Verduzco: Surface wrinkling in liquid crystal elastomers. *Soft Matter* **8**, 7138 (2012).
32. J. Küpfer and H. Finkelmann: Nematic liquid single crystal elastomers. *Macromol. Chem. Rapid Commun.* **12**, 717 (1991).
33. J.E. Mark: *Polymer Data Handbook* (Oxford University Press, New York, USA, 1999).
34. A. Agrawal, T. Yun, S.L. Pesek, W.G. Chapman, and R. Verduzco: Shape-responsive liquid crystal elastomer bilayers. *Soft Matter* **10**, 1411 (2014).
35. I. Komuro, T. Kaida, Y. Shibazaki, M. Kurabayashi, Y. Katoh, E. Hoh, F. Takaku, and Y. Yazaki: Stretching cardiac myocytes stimulates protooncogene expression. *J. Biol. Chem.* **265**, 3595 (1990).
36. T. Yamazaki, I. Komuro, S. Kudoh, Y. Zou, I. Shiojima, T. Mizuno, H. Takano, Y. Hiroi, K. Ueki, and K. Tobe: Mechanical stress activates protein kinase cascade of phosphorylation in neonatal rat cardiac myocytes. *J. Clin. Invest.* **96**, 438 (1995).
37. C. Fink, S. Ergün, D. Kralisch, U. Remmers, J. Weil, and T. Eschenhagen: Chronic stretch of engineered heart tissue induces hypertrophy and functional improvement. *FASEB J.* **14**, 669 (2000).
38. H. Mansour, P.P. de Tombe, A.M. Samarel, and B. Russell: Restoration of resting sarcomere length after uniaxial static strain is regulated by protein kinase C epsilon and focal adhesion kinase. *Circ. Res.* **94**, 642 (2004).
39. J-G. Yu and B. Russell: Cardiomyocyte remodeling and sarcomere addition after uniaxial static strain in vitro. *J. Histochem. Cytochem.* **53**, 839 (2005).
40. M. Chambers, H. Finkelmann, M. Remškar, A. Sánchez-Ferrer, B. Zalar, and S. Žumer: Liquid crystal elastomer–nanoparticle systems for actuation. *J. Mater. Chem.* **19**, 1524 (2009).
41. M. Chambers, B. Zalar, M. Remskar, S. Zumer, and H. Finkelmann: Actuation of liquid crystal elastomers reprocessed with carbon nanoparticles. *Appl. Phys. Lett.* **89**, 243116 (2006).
42. F. Greco, V. Domenici, A. Desii, E. Sinibaldi, B. Zupančič, B. Zalar, B. Mazzolai, and V. Mattoli: Liquid single crystal elastomer/conducting polymer bilayer composite actuator: Modelling and experiments. *Soft Matter* **9**, 11405 (2013).

https://doi.org/10.1557/jmr.2014.392 Published online by Cambridge University Press

43. R.R. Kohlmeyer and J. Chen: Wavelength-selective, IR light-driven hinges based on liquid crystalline elastomer composites. *Angew. Chem., Int. Ed.* **52**, 9234 (2013).
44. S.V. Ahir and E.M. Terentjev: Photomechanical actuation in polymer-nanotube composites. *Nat. Mater.* **4**, 491 (2005).
45. S.V. Ahir, A.M. Squires, A.R. Tajbakhsh, and E.M. Terentjev: Infrared actuation in aligned polymer-nanotube composites. *Phys Rev. B* **73**, 085420 (2006).
46. J.E. Marshall and E.M. Terentjev: Photo-sensitivity of dye-doped liquid crystal elastomers. *Soft Matter* **9**, 8547 (2013).

Supplementary Material

To view the supplementary material for this article, please visit http://dx.doi.org/jmr.2014.392. Supplementary videos of shape-responsive LCEs, data on temperatures measured at 5 and 20 W heating powers, analysis of cellular orientation on wrinkled substrates, and additional images from cell culture experiments are provided in the supplementary information.

https://doi.org/10.1557/jmr.2014.392 Published online by Cambridge University Press